Macromolecules
ARTICLE

Macromolecules **2010**, *43*, 9447–9453 **9447**
DOI: 10.1021/ma101696q

Tailoring Properties of Carbon Nanotube Dispersions and Nanocomposites Using Temperature-Responsive Copolymers of Pyrene-Modified Poly(*N*-cyclopropylacrylamide)

Krishna C. Etika,[†] Florian D. Jochum,[‡] Michael A. Cox,[†] Philipp Schattling,[‡] Patrick Theato,*[,‡,§] and Jaime C. Grunlan*[,†]

[†]*Department of Mechanical Engineering, Texas A&M University, College Station, Texas 77843, United States,* [‡]*Institute of Organic Chemistry, University of Mainz, Mainz, Germany, and* [§]*School of Chemical and Biological Engineering, WCU Program of Chemical Convergence for Energy & Environment (C2E2), College of Engineering, Seoul National University, 151-744 Seoul, Korea*

Received July 27, 2010; Revised Manuscript Received October 8, 2010

ABSTRACT: Despite their immense potential, the ability to control the dispersion and microstructure of carbon nanotubes remains a hurdle for their widespread use. Stimuli-responsive polymers show conformational changes with an applied external stimulus (pH, temperature, light, etc.). The dispersion of carbon nanotubes by thermoresponsive polymers is shown to enable the macroscopic properties of aqueous suspensions to be tailored as a function of temperature. This work presents the synthesis, characterization, and use of temperature-responsive poly(*N*-cyclopropylacrylamide) (PNCPA) polymers containing 1, 3, and 5 mol % pyrene-bearing repeat units to tailor the dispersion state of single-walled carbon nanotubes (SWNT) in water. Turbidity measurements show that the lower critical solution temperature (LCST) of PNCPA decreases with increasing pyrene content. Viscosity measurements on aqueous SWNT suspensions stabilized with pyrene-functionalized PNCPA show highly entangled and well-dispersed nanotube microstructure above and below the LCST of the polymer, respectively. UV−vis spectra also confirm that nanotube stabilization by these polymers is dependent upon the pyrene content. Drying of these suspensions produces composites whose microstructure and electrical conductivity vary with drying temperature and pyrene content of the stabilizing polymer. This temperature-dependent dispersion behavior has significant implications for the processing of carbon nanotubes and tailoring of composite properties. Such stimuli-controlled dispersion of carbon nanotubes could have a variety of applications in nanoelectronics, sensing, and drug and gene delivery systems.

Introduction

Carbon nanotubes are of great interest, both from a fundamental point of view and for practical applications,[1,2] due to their high aspect ratio (often >1000) and conjugated chemical structure. Nanotubes possess attractive mechanical,[3] thermal,[4] and electronic properties[5] that suggest a wide range of application for this material.[6] Furthermore, liquid suspensions of carbon nanotubes specifically have potential for use in biological,[7,8] optical,[9] and sensory devices.[10] Despite all of their promise, very limited progress has been made toward realizing the full potential of nanotubes. One main reason for this lack of success is the difficulty associated with the dispersion of otherwise bundled tubes. As-produced single-walled carbon nanotubes (SWNTs) exist in a highly bundled state because of strong van der Waals attraction that severely limits their dispersion in solvents, especially in water.[11,12] Large-scale utilization of nanotubes not only depends upon production of stable suspensions at high weight fraction but also requires the ability to control the state of nanotube dispersion in these suspensions.[13]

A variety of covalent[14−19] and noncovalent[20−24] modification techniques have been reported for suspending CNTs in various solvents. Covalent functionalization involves the attachment of chemical moieties on the nanotube surface that counteracts the intertube van der Waals force of attraction. The presence of local strain in carbon nanotubes due to pyramidalization and misalignment of the π-orbitals of the sp^2-hybridized carbon atoms makes them more reactive than a flat graphene sheet and thereby eases the attachment of chemical moieties to the surface.[25] A major drawback of covalent functionalization is the disruption of the extended π-conjugation in nanotubes, which degrades electrical properties because each functionalization site scatters electrons.[26,27] On the other hand, noncovalent stabilization involves physical adsorption of polymers or surfactants on the nantube surface.[12] This method of functionalization does not involve breaking bonds in the nanotube sidewalls and therefore better preserves electrical properties.[27−29] For efficient dispersion/solubilization of SWNTs, the above-mentioned methods are often used in conjunction with a mixing technique (e.g., ultrasonication, stirring, etc.).

One type of noncovalent functionalization that has received considerable attention involves the use of pyrene moieties.[30−43] Pyrene is highly aromatic and known to interact strongly with the basal plane of graphite via π-stacking and also interacts strongly with SWNT sidewalls in the same manner.[21] Several pyrene-containing small molecules and polymers have been shown to effectively disperse nanotubes in solvents.[30−43] When these polymers are stimuli-responsive, there is an opportunity to control the dispersion state of nanotubes upon exposure to a given stimulus (e.g., pH, temperature, and/or light) due to conformational

*Corresponding authors. E-mail: theato@uni-mainz.de (P.T.); jgrunlan@tamu.edu (J.C.G.).

Published on Web 10/25/2010

changes in the polymer.[43−45] In many potential applications, such as SWNT-based switching devices, sensors, and drug delivery systems, it may be necessary to control the dispersion or aggregation of SWNTs in solvent with this type of external stimuli.[46]

Thermoresponsive polymers, such as poly(*N*-cyclopropylacrylamide) (PNCPA) and poly(*N*-isopropylacrylamide) (PNIPAM), are a class of stimuli-responsive polymers that show temperature-dependent solubility in water.[30,47−49] These polymers are hydrophilic and soluble in water below their lower critical solution temperature (LCST) but become hydrophobic and insoluble at higher temperatures. The temperature-dependent solubility of these polymers arises from the coil-to-globule conformational transitions of the polymer chains. At temperatures above the LCST, the otherwise "extended" polymer chains collapse to assume a globular conformation, due to extensive intramolecular hydrogen bonding, and becomes immiscible in water.[50] These conformational variations can be used to tailor the nanotube dispersion state in water as a function of temperature.[30,43] Furthermore, copolymerization with hydrophilic or hydrophobic comonomers typically results in an increase or decrease of the LCST, respectively, thereby opening the possibility to precisely tune the LCST of the polymer to fit the desired need.[48]

Earlier studies on aqueous single-walled carbon nanotubes (SWNTs) suspensions, stabilized with 5 mol % pyrene functionalized poly(*N*-cyclopropylacrylamide) (5p-PNCPA), showed thermoresponsive tailoring of nanotube dispersion state.[30] One drawback associated with functionalization of PNCPA, with such a high pyrene content, is the drastic shift in the LCST by more than 20 °C. Lowering the pyrene content in p-PNCPA can offset this shift in LCST but at the same time diminish polymer−nanotube interactions. More recently, it was shown that 1 mol % pyrene-functionalized poly(*N*-isopropylacrylamide) (PNIPAM) exhibits an LCST that is just 4 °C lower than unmodified PNIPAM and stabilizes nanotubes in water.[51] These results highlight the importance of understanding the influence of pyrene content in p-PNCPA to stabilize and/or tailor SWNT dispersion in water as a function of temperature.

In the present work, 1, 3, and 5 mol % pyrene-functionalized PNCPA (1p-PNCPA, 3p-PNCPA, and 5p-PNCPA, respectively) were synthesized to control the dispersion state of SWNTs in water as a function of temperature. Turbidity measurements made on aqueous polymer solutions revealed lowering of LCST with increasing pyrene content in PNCPA. Furthermore, viscosity measurements suggests 5p-PNCPA-stabilized SWNTs suspensions exhibit stronger temperature tailored dispersion state as compared 1p-PNCPA-stabilized nanotubes. UV−vis spectra of suspensions further confirm that nanotube stabilization efficiency of p-PNCPA series is dependent on the pyrene content and improves with increasing pyrene. Studies performed on the dried nanotube suspensions suggest that microstructure in the liquid state is largely preserved in these composites. This method of controlling nanotube microstructure in the solid state can be very useful for solution-processed polymer nanocomposites. Furthermore, tailoring the dispersion state of CNTs in water as a function of temperature could have potential applications in medicine, nanoelectronics, and sensors.

Experimental Section

Materials. All chemicals and solvents are commercially available and used as received unless otherwise stated. Tetrahydrofuran (THF) was distilled over sodium. Spectra/Por 3 (MWCO 3500) were used as dialysis membranes. Poly(pentafluorophenyl acrylate) (PPFPA, **4**) with a molecular weight of 25 000 g/mol (M_w/M_n = 1.32) was synthesized according to a previously reported procedure.[52] Raw single-walled carbon nanotubes (SWNTs) [batch no. R0487] were purchased from Carbon Nanotechnologies (Houston, TX), containing 27 wt % impurity (mostly Fe-based catalyst). These nanotubes were used without further purification. SWNT suspensions were prepared by mixing dry SWNTs in 0.1 wt % aqueous solutions of p-PNCPA, followed by sonication for 10 min at 50 W using a VirTis Virsonic 100 ultrasonic cell disrupter (SP industries, Warminster, PA). Composites of p-PNCPA/SWNT were made by drying 5 mL of suspension on a quartz slide at a given temperature.

Instrumentation. All ^{1}H NMR spectra were collected with a Bruker 300 MHz FT-NMR spectrometer in deuterated solvents. Chemical shifts (δ) were given in ppm relative to TMS. Gel permeation chromatography (GPC) was performed in THF to determine molecular weights and molecular weight distributions (M_w/M_n) of polymer samples with respect to polystyrene standards. Calibration was done using polystyrene standards. UV/vis spectra were recorded on a Jasco V-630 photo spectrometer. Fluorescence measurements were performed on a Perkin-Elmer LS 50B luminescence spectrometer. IR spectra were recorded on a Bruker Vector 22 FT-IR spectrometer using an ATR unit. FD masses were measured on a MAT 95 Finnigan mass spectrometer.

Viscosity of the suspensions as a function of shear rate was measured using an AR-G2 rheometer (TA Instruments, Newcastle, DE) equipped with 40 mm parallel plate geometry. A gap of 1000 μm was maintained as per the recommended procedure for the instrument. This rheometer is equipped with a Peltier control system that provides accurate (±0.1 °C) temperature between 10 and 90 °C. Turbidity measurements were made with a USB2000 UV/vis spectrometer (Ocean Optics, Dunedin, FL) using a quartz cuvette containing 0.1 wt % polymer solution. Scanning electron microscopy was performed with an FEI Quanta 600 FE-SEM on composites coated with a 5 nm layer of Pt/Pd. Sheet resistance of the composites was measured using a custom-built four-point probe apparatus. The details of this instrument and measurement technique have been previously published elsewhere.[53] Volume conductivity was calculated by taking the inverse of the product of the sheet resistance and composite thickness.

Pentafluorophenyl-4-(pyren-1-yl)butanoate (2) Synthesis. 3.00 g (0.010 mol) of 4-(pyren-1-yl)butanoic acid (**1**) and 4.31 mL (0.031 mol) of triethylamine (TEA) were dissolved in 25 mL of dry THF, and 8.74 g (0.031 mol) of pentafluorophenyl trifluoroacetate was added dropwise. The solution was stirred for 12 h at room temperature, then diluted with 300 mL of dichloromethane, and transferred into a separation funnel. The organic phase was washed three times with 50 mL of water, dried with sodium sulfate, and concentrated in vacuum. The product was isolated through precipitation into hexane. After filtration and drying in vacuum at 40 °C, 3.23 g (0.0071 mol, 71%) of yellow pentafluorophenyl-4-(pyren-1-yl)butanoate (**2**) was obtained. ^{1}H NMR ($CDCl_3$) δ /ppm: 8.27 (d, 1H), 8.13 (m, 4H), 8.03 (s, 2H), 7.99 (t, 1H), 7.86 (d, 1H), 3.47 (t, 2H), 2.77 (t, 2H), 2.32 (quin, 2H). FT-IR (ATR-mode): 2944 cm^{-1} (C−H valence), 1774 cm^{-1} (C=O reactive ester band), 1517 cm^{-1} (PFP C=C aromatic band), 1100 cm^{-1} (C−O ester band). MS (FD) m/z (%): 454.3 (100.00), 455.3 (27.58), 456.3 (4.51).

***N*-(6-Aminohexyl)-4-(pyren-1-yl)butanamide (3) Synthesis.** 7.77 g (0.067 mol) of hexamethylenediamine and 0.93 mL (0.0067 mol) of TEA were dissolved in 80 mL of dry THF, and 3.04 g (0.0067 mol) of pentafluorophenyl-4-(pyren-1-yl)butanoate (**2**) dissolved in 30 mL of dry THF was added dropwise. The solution was stirred for 12 h at room temperature, then diluted with 400 mL of dichloromethane, and extracted four times with 80 mL of water. The organic phase was separated and dried with sodium sulfate. After removal of the solvent in vacuum, 2.07 g (0.0054 mol, 80%) of yellow *N*-(6-aminohexyl)-4-(pyren-1-yl)butanamide (**3**) was obtained. ^{1}H NMR (DMSO) δ /ppm: 8.35 (d, 1H), 8.22 (m, 4H), 8.10 (s, 2H),

Scheme 1. Overview of Reactions Used To Synthesize Pyrene-Modified Poly(*N*-cyclopropylacrylamide)

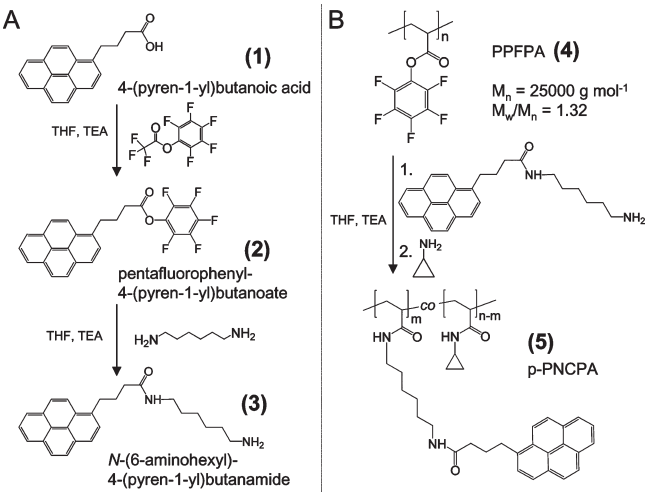

8.02 (t, 1H), 7.90 (d, 1H), 7.83 (t, 1H), 3.29 (t, 2H), 3.06 (q, 2H), 2.46 (t, 2H), 2.24 (t, 2H), 2.00 (quin, 2 H), 1.35 (t, 2H), 1.23 (m, 6H). FT-IR (ATR mode): 3300 cm^{-1} (N−H amide valence), 2928 cm^{-1} (C−H valence), 1643 cm^{-1} (C=O amide band I), 1550 cm^{-1} (C=O amide band II). MS (FD) m/z (%): 386.3 (89.14), 387.4 (58.24), 774.0 (100.00), 775.0 (62.55), 776.0 (3.09).

Synthetic Procedure for Poly(*N*-cyclopropylacrylamide) with Various Amounts of Pyrene Side Groups (p-PNCPA, 5). Three different solutions, each with 2 g of PPFPA (**4**) and 2 mL (0.0143 mol) of TEA dissolved in 20 mL of dry THF, were prepared. Next, 32 mg (8.284×10^{-5} mol for 1p-PNCPA), 97 mg (2.511×10^{-4} mol for 3p-PNCPA), and 162 mg (4.201×10^{-4} mol for 5p-PNCPA) of *N*-(6-aminohexyl)-4-(pyren-1-yl)butanamide (**3**) were added, respectively. The solutions were stirred for 3 h under a nitrogen atmosphere at room temperature. Afterward, 2 mL (0.029 mol) of cyclopropylamine was added to each flask. After stirring for 12 h, the solvent of each reaction sample was removed by evaporation in vacuum. Each residue was suspended in 10 mL of water and dialyzed against diluted ammonia for ~12 h. The clear dialyzed solutions were evaporated, and then the residues were twice dissolved in 5 mL of methanol and precipitated into diethyl ether. After centrifugation and drying in vacuum at 40 °C, between 0.49 and 0.61 g of colorless p-PNCPA polymers containing various amounts of pyrene moieties (1p-PNCPA, 3p-PNCPA, and 5p-PNCPA) was obtained. ^{1}H NMR (MeOD) δ /ppm: 8.13 (m), 3.21 (s), 2.71 (s), 2.38 (s), 2.06 (br s), 1.59 (br s), 0.67 (d). FT-IR (ATR mode): 3280 cm^{-1} (N−H amide valence), 2940 cm^{-1} (C−H valence), 1643 cm^{-1} (C=O amide band I), 1540 cm^{-1} (C=O amide band II). UV/vis (MeOH): λ_{max} = 233, 242, 254, 265, 275, 312, 326, and 342 nm. Fluorescence emission (MeOH, λ_{ex} = 340 nm): λ_{max} = 377, 397, 419, and 475 nm.

Results and Discussion

Poly(*N*-cyclopropylacrylamide) with pyrene moieties (p-PNCPA, **5**) was obtained through a polymer analogous reaction of poly(pentafluorophenyl acrylate) (PPFPA, **4**) with *N*-(6-aminohexyl)-4-(pyren-1-yl)butanamide and cyclopropylamine according to Scheme 1. Previously, *N*-(6-aminohexyl)-4-(pyren-1-yl)butanamide was synthesized in two steps. First, 4-(pyren-1-yl)butanoic acid (**1**) was activated by treatment with pentafluorophenyl trifluoracetate (see Scheme 1). In the following reaction, pentafluorophenyl-4-(pyren-1-yl)butanoate (**2**) was converted with an excess amount of hexamethylenediamine into the amino-functionalized *N*-(6-aminohexyl)-4-(pyren-1-yl)butanamide (**3**). Successful reaction was demonstrated with

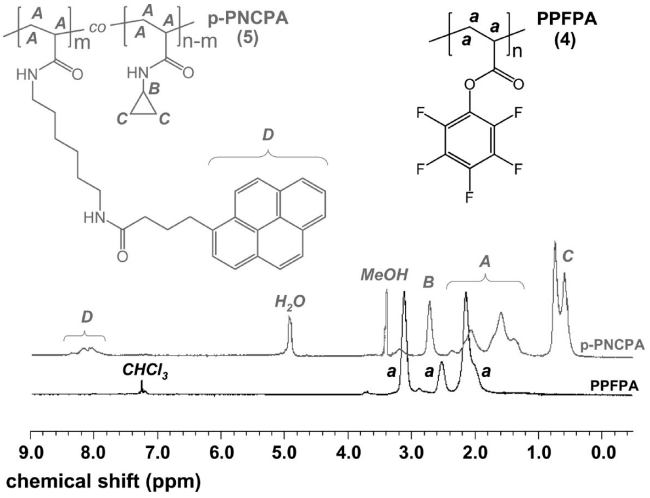

Figure 1. ^{1}H NMR spectra of PPFPA (black line) and p-PNCPA with 5 mol % pyrene moieties (5p-PNCPA, gray line) measured in deuterated solvents $CDCl_3$ and MeOD, respectively.

NMR, FD mass, and IR spectroscopy. Next, the PPFPA (**4**) was synthesized by RAFT polymerization as described earlier.[52] The activated ester polymer (**4**) was then allowed to react with different amounts of *N*-(6-aminohexyl)-4-(pyren-1-yl)butanamide (**3**) and cyclopropylamine at room temperature (see Scheme 1), resulting in p-PNCPA (**5**) copolymers with various amounts (1p-PNCPA, 1 mol %; 3p-PNCPA, 3 mol %; and 5p-PNCPA, 5 mol %) of pyrene side groups.

^{1}H NMR spectroscopy confirmed a successful synthesis of the p-PNCPA copolymer series. The characteristic signals of the aromatic pyrene side groups at 8.13 ppm, as well as the cyclopropylamide repeating units at 2.71 and 0.67 ppm, were assigned as illustrated for 5p-PNCPA in Figure 1. The amount of incorporated pyrene side groups was determined by calculating the ratio of the integrals of the aromatic pyrene protons and the single signal of the cyclopropyl proton at 2.71 ppm. It is noteworthy that the calculated values from NMR measurements fit to the theoretical values, indicating the high accuracy of the polymer analogous reaction.

UV−vis and fluorescence emission spectrum of the p-PNCPA series was collected to investigate the synthesized copolymers, as shown in Figure 2. Both spectra clearly show the characteristic peaks of the pyrene side groups, between 200 and 350 nm for UV−vis and between 350 and 550 nm for fluorescence emission. Furthermore, with increasing pyrene content in PNCPA, UV absorption and fluorescence emission are shown to increase. Greater absorption indicates that more pyrene groups are present in the polymer, as expected by the concentration with which they were incorporated into the polymer.

In an effort to determine the influence of pyrene addition on the LCST of p-PNCPA, turbidity measurements (actually decadic absorbance at 400 nm) were made on dilute aqueous solutions as a function of temperature. These solutions become turbid near the LCST (referred to as the cloud point temperature), which is defined as the temperature corresponding to a 10% reduction in the original transmittance of the solution.[54] Figure 3 shows that the LCST of p-PNCPA in water is dependent on pyrene content and decreases with increasing pyrene content. This reduction of LCST with pyrene addition has been observed by others and is attributed to the increasing hydrophobic character of the polymer.[49,55,56] Tailoring the LCST of PNCPA through incorporation of hydrophobic compounds may actually be desirable for applications requiring a specific transition temperature.

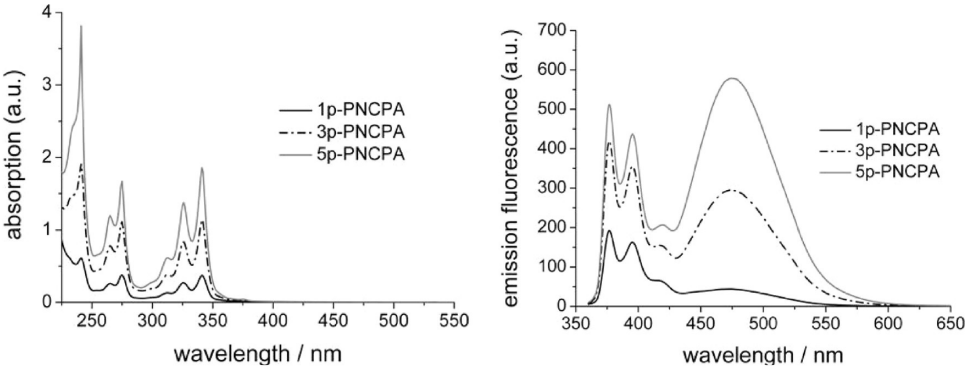

(a) (b)

Figure 2. (a) UV/vis absorption spectra of the p-PNCPA series measured at constant concentration (0.16 mg/mL in methanol) (b) and fluorescence emission spectra (λ_{ex} = 340 nm) of the p-PNCPA series measured at constant concentration (0.0032 mg/mL in methanol).

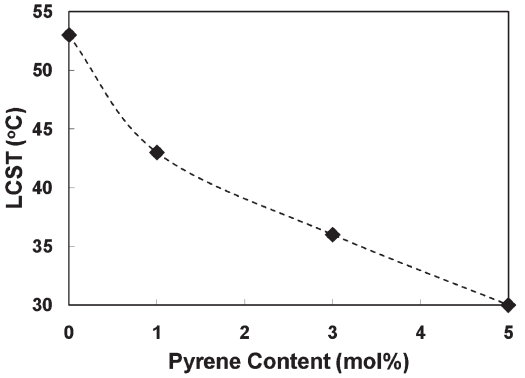

Figure 3. Lower critical solution temperatures of 0.1 wt % solutions of pyrene-functionalized PNCPA as a function of pyrene content.

Viscosity measurements were made both below and above the LCST of the copolymers, as shown in Figure 4, to investigate the nanotube dispersion state in aqueous SWNT suspensions stabilized with pyrene-functionalized PNCPA. It can be seen that both 1p-PNCPA- and 5p-PNCPA-stabilized SWNT suspensions exhibit a shear thinning behavior (i.e., decreasing viscosity with increasing shear) at temperatures above the LCST of the polymer. Furthermore, unmodified PNCPA treated nanotube suspensions are shear thinning both above and below the LCST of the polymer. Shear thinning behavior is observed in concentrated nanotube suspensions that exhibit a high degree of entanglements and resemble polymer-like solutions.[57] With this understanding, it is reasonable to suggest that SWNTs are more networked and entangled above LCST in suspensions stabilized with 5p-PNCPA. It should be noted that below the LCST of the polymer SWNT/5p-PNCPA and SWNT/3p-PNCPA (not shown here) suspensions exhibit nearly Newtonian behavior (shear-independent viscosity) which suggests well-dispersed and exfoliated nanotubes. In contrast, SWNT/1p-PNCPA suspensions also show shear-thinning behavior below LCST, but they exhibit lower viscosities at every shear rate examined. This suggests that 1p-PNCPA is relatively less effective than 5p-PNCPA, but better than unmodified PNCPA, for stabilizing nanotubes. The low pyrene content produces weaker interactions between 1p-PNCPA and SWNTs, as only pyrene moieties can interact with nanotubes through $\pi-\pi$ stacking. Moreover, lower pyrene content will also lead to a lower coverage of polymer on the nanotube sidewalls, thereby reducing the steric hindrance for agglomeration. Similar observations were made with nanotubes stabilized with pyrene-containing block copolymers where higher concentration of pyrene resulted in greater solubility in water.[32]

To further characterize the stability of SWNT suspensions, UV−vis measurements were made on aqueous nanotube suspensions stabilized with the p-PNCPA series, as shown in Figure 5. The carrier dynamics in SWNT bundles are dominated by tunnel coupling between semiconducting and metallic SWNTs, which results in reduced interaction with light that makes nanotube bundles optically inactive.[58−62] With this in mind it is reasonable to suggest that only individual SWNTs can provide a UV−vis signature. This means that greater UV−vis absorbance corresponds to the presence of more exfoliated SWNTs in the suspension. Figure 5a shows SWNT suspensions stabilized with 1p-PNCPA exhibit significantly lower optical absorption, immediately after sonication, as compared to higher pyrene-containing copolymers. This demonstrates the inefficiency of 1p-PNCPA to stabilize aqueous SWNT suspensions. 3p-PNCPA and 5p-PNCPA stabilized SWNTs exhibit similar absorbance to one another in the wavelength range investigated. On the basis of the UV−vis spectra collected after sonication, it appears that both 3p-PNCPA and 5p-PNCPA are equally effective at stabilizing SWNTs. After suspensions were kept standing for 48 h, UV−vis spectra were recollected, as shown in Figure 5b. The optical absorption in SWNT suspensions stabilized with the p-PNCPA series is now more clearly dependent upon pyrene content, increasing with each greater pyrene concentration. The lowering of optical absorption in the 3p-PNCPA-stabilized suspension, as compared to the 5p-PNCPA-stabilized suspension, demonstrates that the former is less stable than the latter. On the basis of these results, it is believed that nanotube stabilization efficiency in these suspensions is directly influenced by pyrene concentration, where higher pyrene-containing polymers stabilize nanotubes better.

It was previously shown that nanotube dispersion state in the liquid suspensions is largely preserved in composites prepared upon drying these suspensions.[30,51,63] In an effort to characterize nanotube microstructure in the liquid state, SWNT suspensions stabilized with pyrene-functionalized PNCPA were dried on glass substrates at temperatures above and below the LCST of the polymer. Scanning electron microscopy (SEM) was performed on these composite films, as shown in Figure 6. It can be seen that nanotube dispersion state in these composites is dependent on temperature. Nanotubes are well dispersed in 1p-PNCPA/SWNT composites dried at a temperature below the LCST of the polymer but exhibit a heavily bundled and networked microstructure in composites made above the LCST. These images indicate that SWNTs are exfoliated and more bundled at temperatures below and above the LCST of 1p-PNCPA, respectively.

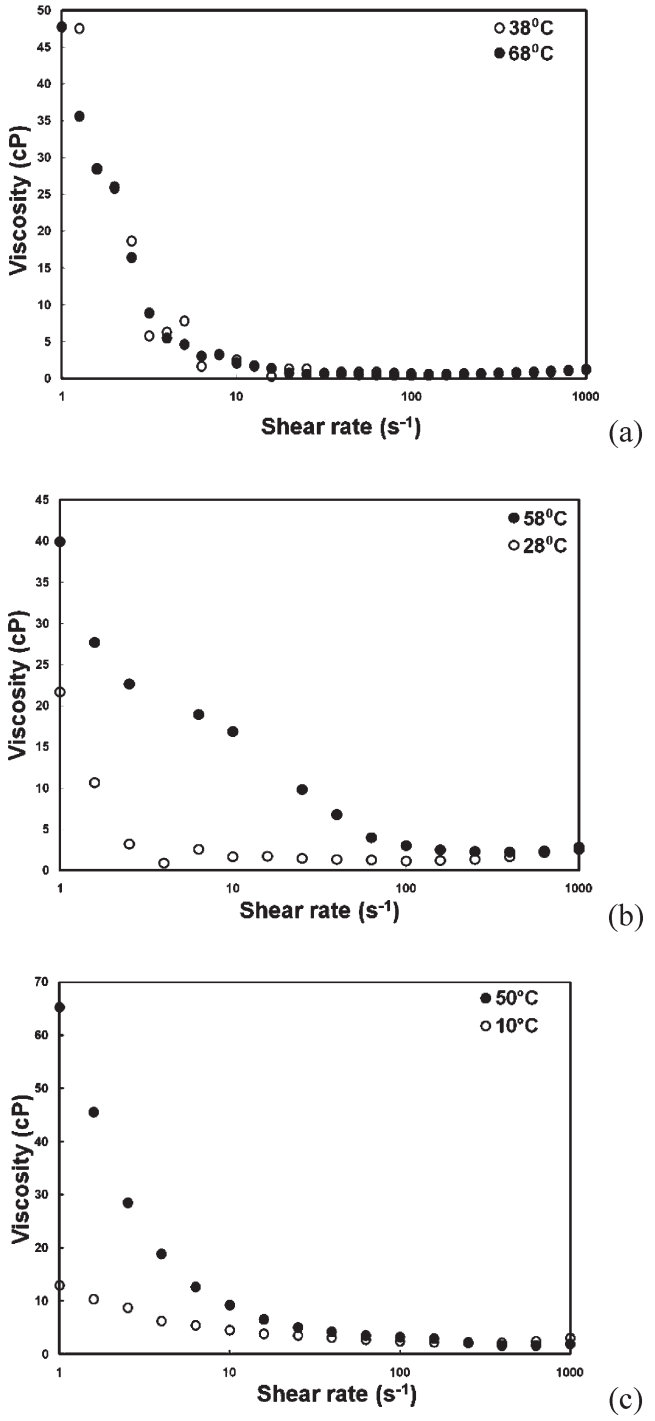

Figure 4. Viscosity as a function of shear rate of 0.011 wt % aqueous SWNT suspensions stabilized by 0.1 wt % of PNCPA (a), 1p-PNCPA (b), and 5p-PNCPA (c), at temperatures below and above the LCST. Graph (c) is reprinted from ref 30.

A similar temperature-dependent dispersion state is also seen in 5p-PNCPA/SWNT composites. The presence of more aggregated nanotube microstructure in 1p-PNCPA composites, as compared to 5p-PNCPA composites dried below the LCST, should be noted. These images compliment the viscosity data (Figure 4) and suggest that SWNTs are better stabilized by 5p-PNCPA than 1p-PNCPA at temperatures below the LCST. As already mentioned, this improved stabilization is attributed to greater pyrene content of 5p-PNCPA. This method of controlling the nanotube dispersion state in solid composites with drying temperature could be a useful tool for tailoring

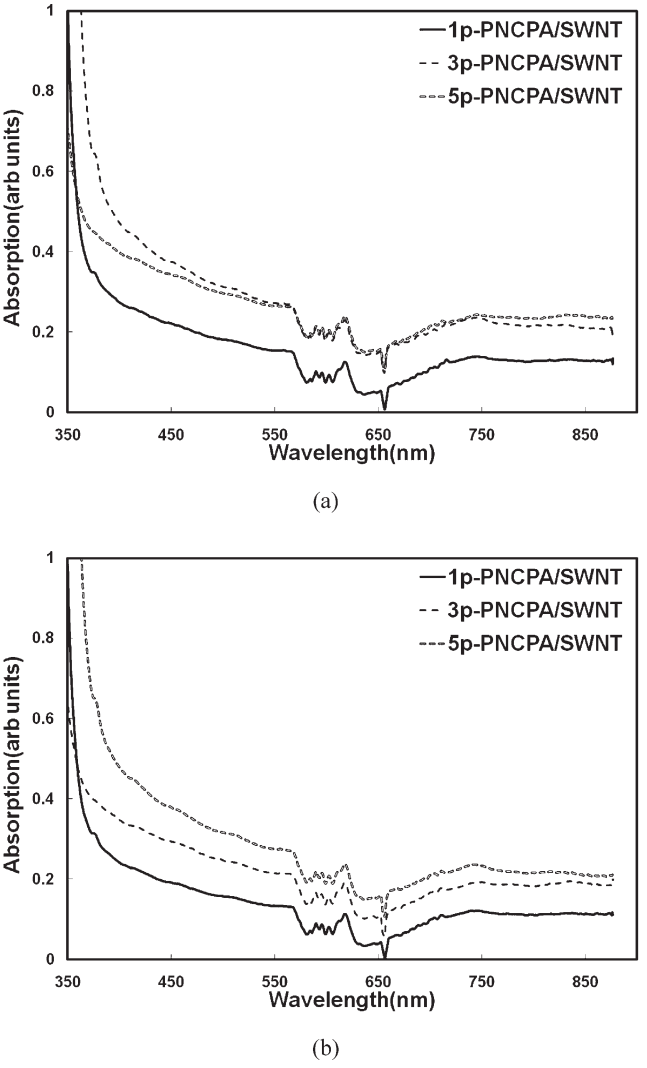

Figure 5. UV−Vis spectra of aqueous suspensions containing 0.0011 wt % SWNT and 0.01 wt % polymer after sonication (a) and 48 h after sonication (b).

the behavior of solution-processed nanotube-filled polymer composites.

To further characterize the solid-state microstructure, electrical conductivity measurements were made on the dried suspensions. It can be seen from Figure 7 that suspensions dried at temperatures above the LCST exhibit significantly higher electrical conductivity than those dried at lower temperatures. This increased electrical conductivity is attributed to a greater number of nanotube−nanotube contacts in these composites. The suspensions above the LCST of the polymer exhibit a highly entangled nanotube microstructure that is preserved upon drying and results in a greater number of tube−tube contacts. In contrast, the suspensions below the LCST have better dispersed (and debundled) nanotubes that have fewer connections with each other, resulting in lower composite electrical conductivity. It can also be seen from Figure 7 that electrical conductivity decreases with increasing pyrene content of PNCPA in these composites. Moreover, this decrease in conductivity is more significant in films made at temperatures above the LCST. Greater interaction between the polymer and nanotube with increasing pyrene content may account for this behavior. The association of polymer with nanotube acts as a barrier to electron movement by shielding the nanotube surface, leading to a lower number of contacts, which results in decreased

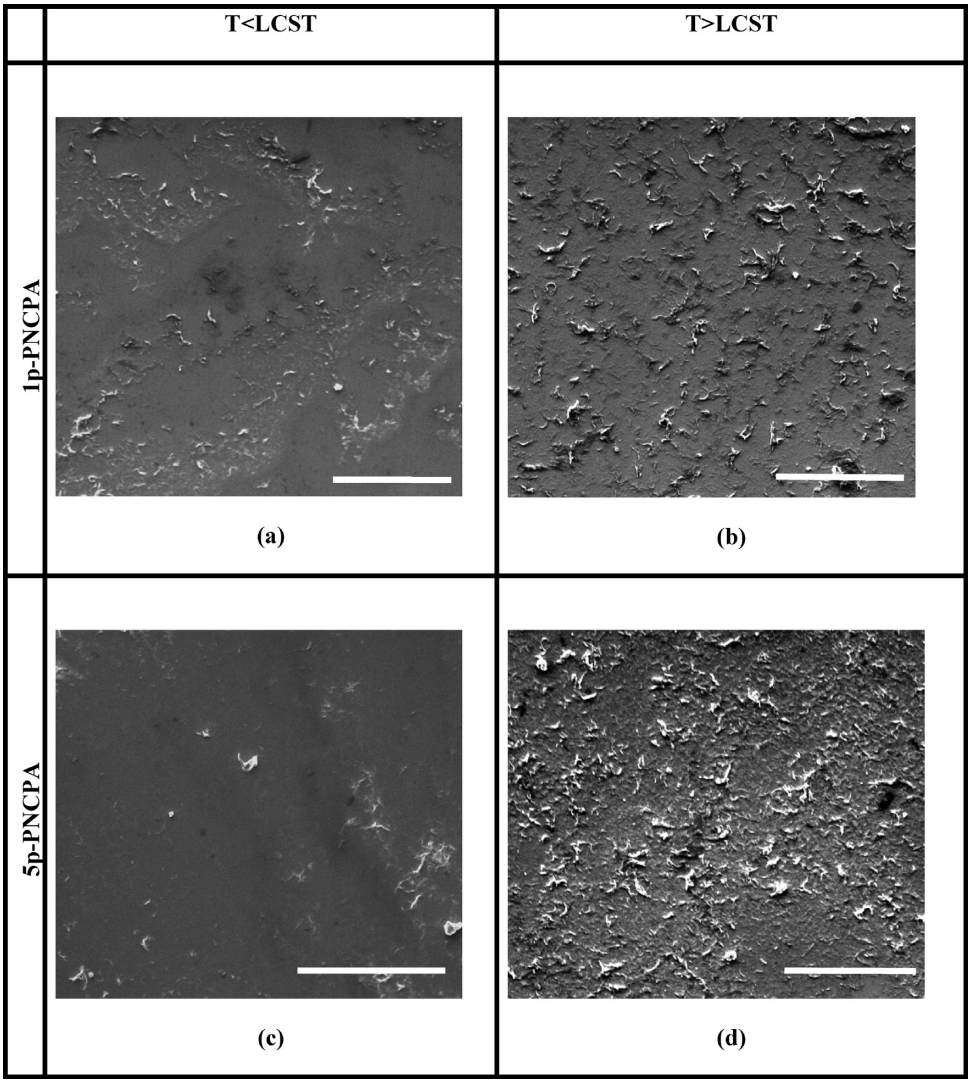

Figure 6. Surface SEM images of 1p-PNCPA (a, b) and 5p-PNCPA (c, d) composites containing 1 wt % SWNTs at temperatures below (left) and above (right) the LCST of the polymer. The scale bar is 20 μm.

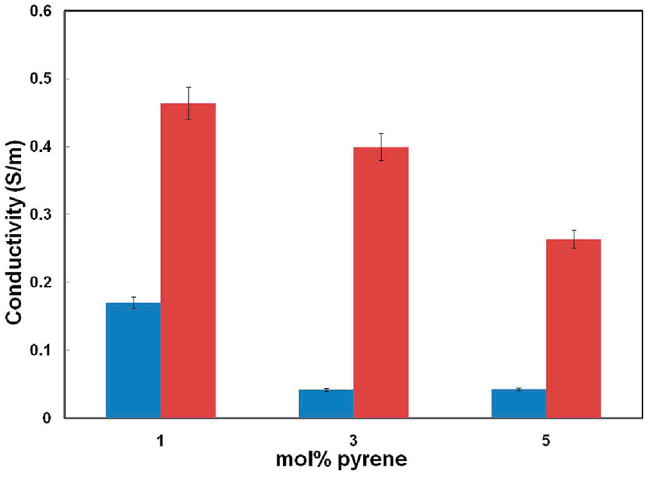

Figure 7. Electrical conductivity of 10 wt % SWNT in pyrene-functionalized PNCPA composites, made at temperatures below (blue) and above (red), the LCST, as a function of pyrene concentration.

electrical conductivity. It was shown that noncovalently functionalized nanotubes exhibit lower electrical conductivities than pristine nanotubes.[64]

Conclusions

In an effort to investigate the influence of pyrene addition on the temperature-responsive characteristics of PNCPA, varying mol % pyrene-functionalized PNCPA were synthesized. Turbidity measurements indicate that LCST in these polymers decreases with increasing pyrene concentration. These polymers were then used to stabilize SWNTs in water, and viscosity measurements suggest that nanotubes in these suspensions exhibit a temperature-dependent dispersion state. At a temperature below LCST, the nanotubes are well dispersed, and at higher temperature they are more entangled. Viscosity and UV−vis spectroscopy confirm that greater pyrene content results in improved nanotube stabilization/dispersion. Composites made by drying these suspensions suggest that nanotube microstructure in the liquid state is preserved to a large extent in the solid state, as evidenced by SEM images and electrical conductivity. This method of controlling nanotube dispersion state in water to influence the properties of solid-state composites will be very useful for the synthesizing nanotube−polymer composites with tailorable properties.

References and Notes

(1) Baughman, R. H.; Zakhidov, A. A.; de Heer, W. A. *Science* **2002**, *297*, 787.

(2) Ouyang, M.; Huang, J. L.; Lieber, C. M. *Acc. Chem. Res.* **2002**, *35*, 1018.
(3) Salvetat, J. P.; Briggs, G. A. D.; Bonard, J. M.; Bacsa, R. R.; Kulik, A. J.; Stockli, T.; Burnham, N. A.; Forro, L. *Phys. Rev. Lett.* **1999**, *82*, 944.
(4) Berber, S.; Kwon, Y. K.; Tomanek, D. *Phys. Rev. Lett.* **2000**, *84*, 4613.
(5) Odom, T. W.; Huang, J. L.; Kim, P.; Lieber, C. M. *Nature* **1998**, *391*, 62.
(6) Terrones, M. *Annu. Rev. Mater. Res.* **2003**, *33*, 419.
(7) Kam, N. W. S.; Liu, Z. A.; Dai, H. J. *Angew. Chem., Int. Ed.* **2006**, *45*, 577.
(8) Douroumis, D.; Fatouros, D. G.; Bouropoulos, N.; Papagelis, K.; Tasis, D. *Int. J. Nanomed.* **2007**, *2*, 761.
(9) Mishra, S. R.; Rawat, H. S.; Mehendale, S. C.; Rustagi, K. C.; Sood, A. K.; Bandyopadhyay, R.; Govindaraj, A.; Rao, C. N. R. *Chem. Phys. Lett.* **2000**, *317*, 510.
(10) Barone, P. W.; Baik, S.; Heller, D. A.; Strano, M. S. *Nature Mater.* **2005**, *4*, 86.
(11) Zheng, M.; Jagota, A.; Semke, E. D.; Diner, B. A.; Mclean, R. S.; Lustig, S. R.; Richardson, R. E.; Tassi, N. G. *Nature Mater.* **2003**, *2*, 338.
(12) Ajayan, P. M.; Tour, J. M. *Nature* **2007**, *447*, 1066.
(13) Islam, M. F.; Rojas, E.; Bergey, D. M.; Johnson, A. T.; Yodh, A. G. *Nano Lett.* **2003**, *3*, 269.
(14) Chen, J.; Hamon, M. A.; Hu, H.; Chen, Y. S.; Rao, A. M.; Eklund, P. C.; Haddon, R. C. *Science* **1998**, *282*, 95.
(15) Khabashesku, V. N.; Billups, W. E.; Margrave, J. L. *Acc. Chem. Res.* **2002**, *35*, 1087.
(16) Bahr, J. L.; Yang, J. P.; Kosynkin, D. V.; Bronikowski, M. J.; Smalley, R. E.; Tour, J. M. *J. Am. Chem. Soc.* **2001**, *123*, 6536.
(17) Coleman, K. S.; Bailey, S. R.; Fogden, S.; Green, M. L. H. *J. Am. Chem. Soc.* **2003**, *125*, 8722.
(18) Liang, F.; Sadana, A. K.; Peera, A.; Chattopadhyay, J.; Gu, Z. N.; Hauge, R. H.; Billups, W. E. *Nano Lett.* **2004**, *4*, 1257.
(19) Park, H. J.; Kim, J.; Chang, J. Y.; Theato, P. *Langmuir* **2008**, *24*, 10467.
(20) Bandow, S.; Rao, A. M.; Williams, K. A.; Thess, A.; Smalley, R. E.; Eklund, P. C. *J. Phys. Chem. B* **1997**, *101*, 8839.
(21) Chen, R. J.; Zhang, Y. G.; Wang, D. W.; Dai, H. J. *J. Am. Chem. Soc.* **2001**, *123*, 3838.
(22) Star, A.; Stoddart, J. F.; Steuerman, D.; Diehl, M.; Boukai, A.; Wong, E. W.; Yang, X.; Chung, S. W.; Choi, H.; Heath, J. R. *Angew. Chem., Int. Ed.* **2001**, *40*, 1721.
(23) Chen, R. J.; Bangsaruntip, S.; Drouvalakis, K. A.; Kam, N. W. S.; Shim, M.; Li, Y. M.; Kim, W.; Utz, P. J.; Dai, H. J. *Proc. Natl. Acad. Sci. U.S.A.* **2003**, *100*, 4984.
(24) Huang, W. J.; Fernando, S.; Allard, L. F.; Sun, Y. P. *Nano Lett.* **2003**, *3*, 565.
(25) Niyogi, S.; Hamon, M. A.; Hu, H.; Zhao, B.; Bhowmik, P.; Sen, R.; Itkis, M. E.; Haddon, R. C. *Acc. Chem. Res.* **2002**, *35*, 1105.
(26) Dyke, C. A.; Tour, J. M. *J. Phys. Chem. A* **2004**, *108*, 11151.
(27) Liu, L.; Etika, K. C.; Liao, K. S.; Hess, L. A.; Bergbreiter, D. E.; Grunlan, J. C. *Macromol. Rapid Commun.* **2009**, *30*, 627.
(28) Chen, J.; Liu, H. Y.; Weimer, W. A.; Halls, M. D.; Waldeck, D. H.; Walker, G. C. *J. Am. Chem. Soc.* **2002**, *124*, 9034.
(29) O'Connell, M. J.; Boul, P.; Ericson, L. M.; Huffman, C.; Wang, Y. H.; Haroz, E.; Kuper, C.; Tour, J.; Ausman, K. D.; Smalley, R. E. *Chem. Phys. Lett.* **2001**, *342*, 265.
(30) Etika, K. C.; Jochum, F. D.; Theato, P.; Grunlan, J. C. *J. Am. Chem. Soc.* **2009**, *131*, 13598.
(31) Meuer, S.; Braun, L.; Zentel, R. *Chem. Commun.* **2008**, 3166.
(32) Bahun, G. J.; Wang, C.; Adronov, A. *J. Polym. Sci., Part A: Polym. Chem.* **2006**, *44*, 1941.
(33) Ehli, C.; Rahman, G. M. A.; Jux, N.; Balbinot, D.; Guldi, D. M.; Paolucci, F.; Marcaccio, M.; Paolucci, D.; Melle-Franco, M.; Zerbetto, F.; Campidelli, S.; Prato, M. *J. Am. Chem. Soc.* **2006**, *128*, 11222.
(34) Wang, D.; Ji, W. X.; Li, Z. C.; Chen, L. W. *J. Am. Chem. Soc.* **2006**, *128*, 6556.
(35) Guldi, D. M.; Rahman, G. M. A.; Jux, N.; Balbinot, D.; Hartnagel, U.; Tagmatarchis, N.; Prato, M. *J. Am. Chem. Soc.* **2005**, *127*, 9830.
(36) Yuan, W. Z.; Mao, Y.; Zhao, H.; Sun, J. Z.; Xu, H. P.; Jin, J. K.; Zheng, Q.; Tang, B. Z. *Macromolecules* **2008**, *41*, 701.
(37) Kimura, M.; Miki, N.; Suzuki, D.; Adachi, N.; Tatewaki, Y.; Shirai, H. *Langmuir* **2009**, *25*, 776.
(38) Assali, M.; Leal, M. P.; Fernandez, I.; Baati, R.; Mioskowski, C.; Khiar, N. *Soft Matter* **2009**, *5*, 948.
(39) Prencipe, G.; Tabakman, S. M.; Welsher, K.; Liu, Z.; Goodwin, A. P.; Zhang, L.; Henry, J.; Dai, H. J. *J. Am. Chem. Soc.* **2009**, *131*, 4783.
(40) Simmons, T. J.; Bult, J.; Hashim, D. P.; Linhardt, R. J.; Ajayan, P. M. *ACS Nano* **2009**, *3*, 865.
(41) Ogoshi, T.; Takashima, Y.; Yamaguchi, H.; Harada, A. *J. Am. Chem. Soc.* **2007**, *129*, 4878.
(42) Liu, Y.; Yu, Z. L.; Zhang, Y. M.; Guo, D. S.; Liu, Y. P. *J. Am. Chem. Soc.* **2008**, *130*, 10431.
(43) Chen, G.; Wright, P. M.; Geng, J.; Mantovani, G.; Haddleton, D. M. *Chem. Commun.* **2008**, 1097.
(44) Galaev, I. Y.; Mattiasson, B. *Trends Biotechnol.* **1999**, *17*, 335.
(45) Nath, N.; Chilkoti, A. *Adv. Mater.* **2002**, *14*, 1243.
(46) Barone, P. W.; Strano, M. S. *Angew. Chem., Int. Ed.* **2006**, *45*, 8138.
(47) Wang, X. H.; Qiu, X. P.; Wu, C. *Macromolecules* **1998**, *31*, 2972.
(48) Schild, H. G. *Prog. Polym. Sci.* **1992**, *17*, 163.
(49) Jochum, F. D.; zur Borg, L.; Roth, P. J.; Theato, P. *Macromolecules* **2009**, *42*, 7854.
(50) Inomata, H.; Goto, S.; Saito, S. *Macromolecules* **1990**, *23*, 4887.
(51) Etika, K. C.; Jochum, F. D.; Cox, M. A.; Schattling, P.; Theato, P.; Grunlan, J. C. *Macromol. Rapid Commun.* **2010**, *31*, 1368.
(52) Eberhardt, M.; Theato, P. *Macromol. Rapid Commun.* **2005**, *26*, 1488.
(53) Etika, K. C.; Liu, L.; Hess, L. A.; Grunlan, J. C. *Carbon* **2009**, *47*, 3128.
(54) Boutris, C.; Chatzi, E. G.; Kiparissides, C. *Polymer* **1997**, *38*, 2567.
(55) Jochum, F. D.; Theato, P. *Polymer* **2009**, *50*, 3079.
(56) Taylor, L. D.; Cerankowski, L. D. *J. Polym. Sci., Part A: Polym. Chem.* **1975**, *13*, 2551.
(57) Shaffer, M. S. P.; Windle, A. H. *Macromolecules* **1999**, *32*, 6864.
(58) Grossiord, N.; Loos, J.; Meuldijk, J.; Regev, O.; Miltner, H. E.; Van Mele, B.; Koning, C. E. *Compos. Sci. Technol.* **2007**, *67*, 778.
(59) Grossiord, N.; Regev, O.; Loos, J.; Meuldijk, J.; Koning, C. E. *Anal. Chem.* **2005**, *77*, 5135.
(60) Hamada, N.; Sawada, S.; Oshiyama, A. *Phys. Rev. Lett.* **1992**, *68*, 1579.
(61) Saito, R.; Fujita, M.; Dresselhaus, G.; Dresselhaus, M. S. *Appl. Phys. Lett.* **1992**, *60*, 2204.
(62) Kataura, H.; Kumazawa, Y.; Maniwa, Y.; Umezu, I.; Suzuki, S.; Ohtsuka, Y.; Achiba, Y. *Synth. Met.* **1999**, *103*, 2555.
(63) Etika, K. C.; Cox, M. A.; Grunlan, J. C. *Polymer* **2010**, *51*, 1761.
(64) Li, X.; Wong, S. Y.; Tjiu, W. C.; Lyons, B. P.; Oh, S. A.; Bin He, C. *Carbon* **2008**, *46*, 829.